

Subatmospheric pool boiling of water at very low liquid levels

TOMASZ HALON*
DOMINIKA KACZMAREK
WIKTORIA LADA
BARTOSZ ZAJĄCZKOWSKI

Wroclaw University of Science and Technology, Department of Thermal Sciences, Wybrzeże Wyspiańskiego 27, 50-370 Wroclaw, Poland

Abstract The paper discusses how the vapour bubbles growing during boiling under the near-triple point pressure influence the heat transfer coefficient when the refrigerant level is lower than the bubble departure diameter. The experiments were carried out for liquid levels of 0.57 to 1.89 cm, saturated pressure range between 0.9 and 4 kPa (saturation temperatures between 5.5 and 29°C). Boiling occurred on a plain surface with wall heat flux densities between 0.43 and 5.93 Wcm⁻². We determined boiling curves for the low-pressure process and analyzed the changes in wall superheat for different filling levels. The experimentally obtained heat transfer coefficient (HTC) was compared with the theoretical values produced by the most popular mathematical expressions used at higher pressures. We also prepared the boiling map, where we specified two boiling regimes: the regime of convection or small popping bubbles and the regime of isolated bubbles. The results indicate that the level of liquid can be neglected within the heat flux range analyzed in this study. The main mechanism of heat transfer under measured conditions is heat convection and conduction, rather than evaporation. The experimentally determined difference between the heat transfer coefficients for different levels of liquid is under 100 Wm⁻²K⁻¹ (for the same heat flux and pressure at the wall).

Keywords: Pool boiling; Subatmospheric boiling; Water; Boiling heat transfer

*Corresponding Author. Email: tomasz.halon@pwr.edu.pl

Nomenclature

A	–	area, m^2
c_p	–	specific heat, $\text{Jkg}^{-1}\text{K}^{-1}$
d	–	diameter, m
H	–	height, m
h	–	heat transfer coefficient, $\text{Wm}^{-2}\text{K}^{-1}$
Ja	–	Jakob number
Ja^*	–	modified Jakob number
k	–	heat conductivity, $\text{Wm}^{-1}\text{K}^{-1}$
L_c	–	characteristic length, m
MAD	–	mean absolute deviation
p	–	pressure, kPa
Q	–	heat, J
\dot{q}	–	heat flux, Wcm^{-2}
T	–	temperature, K
V	–	volume, m^3

Greek symbols

Δ	–	increment
Δh	–	enthalpy difference, Jkg^{-1}
ΔT	–	superheat, K
λ	–	thermal conductivity, $\text{Wm}^{-1}\text{K}^{-1}$
ρ	–	density, kgm^{-3}

Subscripts and superscripts

amb	–	ambient
app	–	applied value
crit	–	critical
h	–	heater
l	–	liquid
plate	–	heating plate
sat	–	saturation
v	–	vapour
wall	–	wall

1 Introduction

The refrigeration industry is gradually moving towards systems that have a more neutral impact on the environment. This shift is a response to international regulations that govern the maximum allowable global warming potential (GWP) of working fluids. The consequence is the resurgence of natural refrigerants, such as hydrocarbons, carbon dioxide, ammonia, and most importantly water. In terms of safety, water is an outlier in the group.

It is easy to dispose of and does not require additional safety measures during service. The main challenges arise from the fact that as a refrigerant it needs to evaporate at subatmospheric pressures, typically ranging from 1–4 kPa. Sikora and Bohdal highlighted the frequent use of low-pressure refrigerants, such as Novec 649 [1]. Under such conditions, its specific volume increases approximately 70 times, presenting significant difficulties for the design and operation of the evaporator [2]. For this reason, evaporators in chillers are often shell-and-tube or falling-film types [3, 4], which are characterised by a large internal volume and heat transfer surface. However, this also means a large thermal mass that decreases the efficiency of such devices [5].

Another crucial parameter that affects the heat transfer performance is the level of the liquid above the heating surface. Hydrostatic pressure becomes significant at very low operating pressures because it is of a similar magnitude as the saturated pressure. The result is an increase in the temperature of evaporation at the boiling surface and steep temperature and pressure gradients within the liquid volume. Various authors [6, 7] studied how the liquid level affects the nucleation, growth, and departure of the bubble under subatmospheric conditions, highlighting the difference between saturation temperatures at the top and bottom of the bubble. At a few kPa, the liquid level affects the wall temperature due to the cyclic flow of highly subcooled water to the nucleation site (the so-called return flow) [8].

Most studies have concentrated on liquid levels high enough to observe the growth and detachment of bubbles at low pressures (typically > 10 cm). This study builds on our previous research, in which we analysed higher liquid levels and superheat values (10 K or more) [9, 10]. In this paper, we examine the thermal effect of extremely low refrigerant levels, ranging from 0.57 to 1.89 cm. This research focuses on reduced heat flux density at lower liquid levels and its impact on producing lower superheats, which correspond to conditions found in both flooded evaporators and the bottom section of falling-film evaporators.

2 Setup and procedure

2.1 Experimental setup

The experimental test facility is constituted by a 7.7 cm inner diameter stainless-steel cylinder 3 mm thick, filled with distilled water (refrigerant), which is shown in Fig. 1. At the bottom of the cylinder, there is a brass disk

that is connected to an electric heating coil, which is the boiling surface. Its roughness was determined using a contact profilometer at five locations. The mean roughness is 0.0659 cm, mean roughness depth is equal to 4.675 and maximum roughness depth is 8.36. The profilometer length of travel and cut-off length are 0.175 cm and 0.025 cm, respectively.

The electrical power, which is supplied to the coil, is regulated with an autotransformer and measured with an analogue wattmeter (Class I). The evaporation pressure is maintained constant through the effect of the condenser, which is a copper coil. The brass plate that supports the condenser is the top cover of this cylinder. The subatmospheric pressure in the experimental system is obtained by means of a vacuum pump, and the vacuum level is measured with a pressure transducer of 0.1% full scale accuracy. K-type thermocouples connected to a recorder were used to measure temperature. 1 mm below the measured surface, there is a K-type (class I) thermocouple (± 0.5 K after calibration), which is used for wall temperature measurements. The temperature of the heating surface is calculated from the heat conduction equation assuming 1D heat flow and a constant wall material heat conductivity. Stable boiling conditions are obtained by insulating the cylinder with 2 cm thick polyethylene foam on the walls and 80 mm wool on the top and bottom covers.

2.2 Experimental procedure

In this experimental study, two liquid levels were tested, 1.89 and 0.57 cm, which correspond to volumes of 100 and 30 ml, respectively. In the tested experimental stand (shown in Fig. 1), it was easier to measure the volume of water and from it calculate the given height than to measure the height directly. During each series of experiments, the heat transfer surface was rubbed by a microfiber cloth with isopropyl alcohol and after that, the vessel was sealed at the atmospheric pressure. The next test stand was filled with the refrigerant. Low pressure conditions of 2 kPa absolute pressure were obtained by a vacuum pump. The refrigerant started to boil because its temperature was higher than the saturation temperature. After reaching the equilibrium conditions, the vessel was further evacuated to remove any non-condensable gases dissolved in water. Then, it was kept for 24 h for further degassing, after which it was again evacuated by the vacuum pump.

An autotransformer was used to set the heat fluxes (HF). The stabilization process of HF lasted 60 minutes, after which both the pressure inside the vessel and the temperature of the heating wall were recorded.

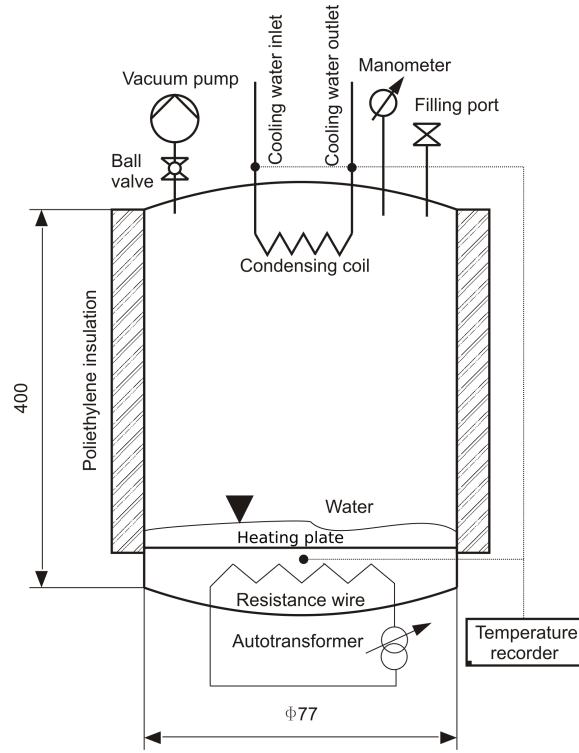


Figure 1: Experimental setup used for the analysis of pool boiling at different levels of refrigerant filling at subatmospheric pressures.

The heat transfer coefficient HTC was calculated using Newton's law of cooling:

$$q = \frac{Q}{A} = \text{HTC} (T_{\text{wall}} - T_{\text{sat}}). \quad (1)$$

The vessels heat load was calculated from the heat balance – heat conduction through 3 mm stainless steel and 20 mm polyurethane foam. The ambient temperature was 19°C, while the temperature inside the vessel ranged from 6 to 27°C. The heat applied by the heating plate Q_{plate} was the heat from electric heater Q_h reduced by the heat loss from the heater to the ambient air Q_{amb} :

$$Q_{\text{plate}} = Q_h - Q_{\text{amb}}. \quad (2)$$

The CoolProp open-source thermodynamic properties library [11] was used to calculate the saturation temperature T_{sat} and other thermodynamic

properties of water. The finite differential method was used to calculate the uncertainty of the heat transfer coefficient measurement. The errors were in the range of 12 to 20% of the estimated HTC value. Experiments were conducted for nine different heat fluxes \dot{q} (0.43, 0.64, 1.07, 1.5, 2.14, 2.58, 3.44, 4.3, and 5.93 Wcm⁻²) and for a pressure range of 0.9 to 4 kPa, which corresponds to saturation temperatures from 5.5°C to 29°C.

3 Results and discussion

The analysis is threefold. First, boiling curves ($\dot{q}(\Delta T)$ plots) were determined for water at pressures of 1.3 kPa and 2.55 kPa for two different liquid levels: 0.57 cm and 1.89 cm. Subsequently, the impact of water level on wall superheat was recorded as a function of time to determine its effect on transient behaviour throughout bubble nucleation. Lastly, the impact of filling level on the heat transfer coefficient as a function of pressure was analyzed. For clarity, the presented results always include the hydrostatic head: 56 Pa and 185 Pa for 0.57 cm and 1.89 cm, respectively.

3.1 Determination of the boiling curve

Figure 2 shows boiling curves for the analyzed refrigerant pressures and liquid levels compared to the already known Nukiyama curve, which was obtained at 1 bar [12]. Each measurement point in the graphs is an averaged value, which was acquired from 3 to 5 measurements.

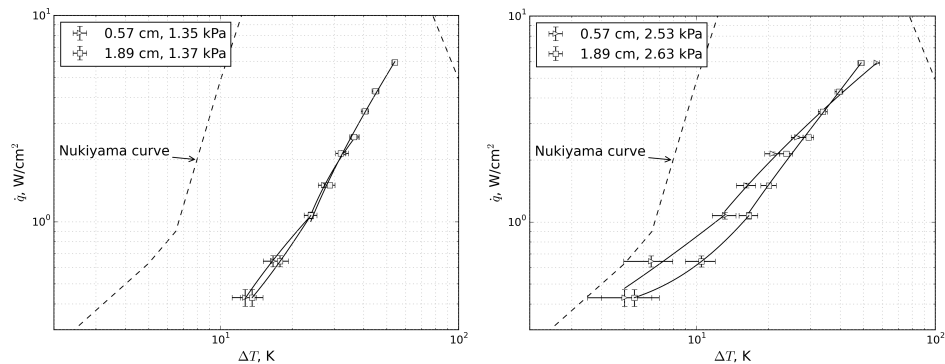


Figure 2: Boiling curves for two liquid levels 0.57 cm and 1.89 cm at two pressure levels: 1.35–1.37 kPa (left) and 2.53–2.63 kPa (right).

The refrigerant level affects boiling curves when the pressure increases from 1.3 to 2.5 kPa. For pressures of 1.3 kPa and with wall heat fluxes in the range of 0.43 Wcm^{-2} to 5.93 Wcm^{-2} , this effect is negligible as in Fig. 2 (left side), but at higher pressures ($\sim 2.5 \text{ kPa}$), the impact of liquid level changes the wall superheat ΔT of the transition point, as in Fig. 2 (right side).

Particularly in the convective boiling region, where the liquid motion due to the bubble nucleation and departure does not occur, a lower liquid level means lower thermal resistance and, compared to work by Schnabel *et al.* [3], this behaviour is different because, in their work, the difference was observed in the nucleate boiling region. The mentioned authors found that regardless of the degree of superheat, more heat was transferred to the liquid at a higher refrigerant filling level. They also suggested that this behaviour was likely due to their test stand, where the circulation of secondary refrigerant in the spaces between the vessel wall and the heating sample affected the heat transfer. Our test stand was more compact, so the circulation of secondary refrigerant was hindered.

As the pressure decreases, the need for a higher superheat for nucleation increases, as shown in Fig. 2. The same phenomenon was also observed in the literature, [3, 10, 13–15]. For a pressure of 1.3 kPa, the beginning of nucleate boiling occurred at superheat $\Delta T = 20 \text{ K}$, while for a pressure of 2.5 kPa at $\Delta T = 10.5 \text{ K}$. For both pressures, the transition took place at the same heat flux of about 1 Wcm^{-2} . It was also observed that the liquid level did not significantly affect superheat, as the peak difference in wall superheat for various refrigerant levels was 7%.

Giraud *et al.* [8] investigated the phenomenon of change in size of vapour bubbles, with decreasing subatmospheric pressure of water. They compared bubble growth before detachment and noted that as the pressure decreases, the bubble diameter increases up to a pressure of 1.8 kPa, below that point the diameter decreases again. Thus, it is possible for the experiments that the detachment bubble diameters for 1.3 kPa and 2.5 kPa are similar. This results in comparable wall superheat values at the highest heat fluxes for both 1.3 and 2.5 kPa pressures.

3.2 Wall superheat

The wall superheat is an indicator of the boiling regime. Its fluctuations indicate the presence of unsteady processes near the wall, such as bubble nucleation or fluid motion. Figure 3a. depicts the relation between the wall

superheat and time, which is crucial to estimate the total heat transfer during nucleate boiling. To mathematically model the heat transfer process during boiling, the frequencies of bubble departure and wall superheat were used.

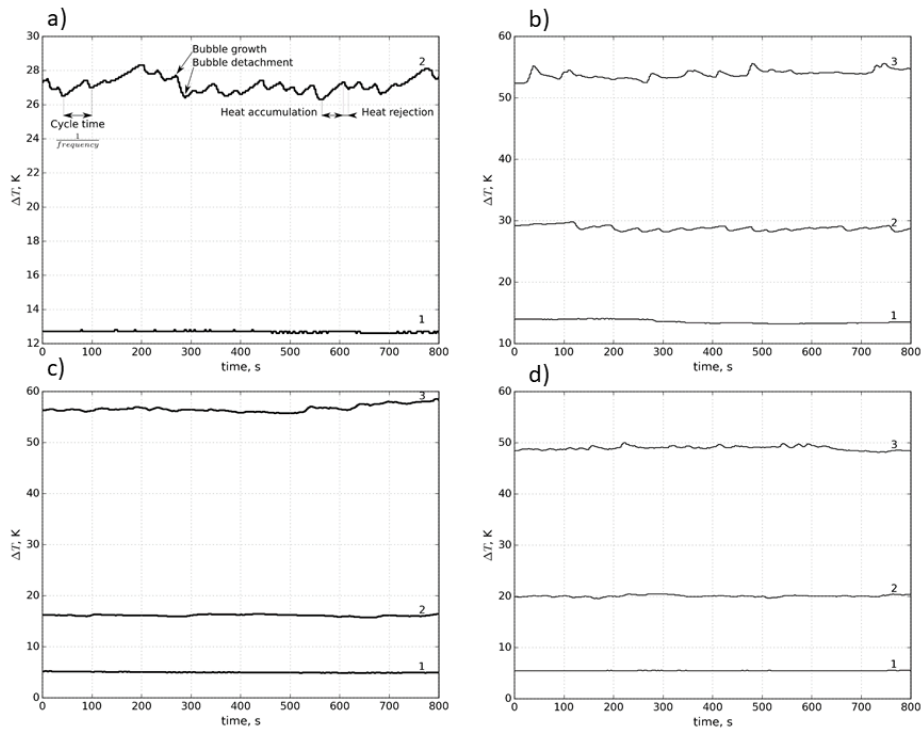


Figure 3: Wall superheat fluctuations for different heat transfer densities: 1 – 0.43 Wcm^{-2} , 2 – 1.5 Wcm^{-2} , 3 – 5.93 Wcm^{-2} ; (a) $p = 1.3 \text{ kPa}$ and 0.57 cm filling, (b) $p = 1.3 \text{ kPa}$ and 1.89 cm filling, (c) $p = 2.5 \text{ kPa}$ and 0.57 cm filling, (d) $p = 2.5 \text{ kPa}$ and 1.89 cm filling.

The heat transfer rate is dependent on a bubble creation rate and departure time. The smaller the bubble creation rate and shorter the departure time (yielding high frequency), the higher the heat transfer rate. For the investigated values of pressures and liquid levels, the amplitude of fluctuations at the lowest heat fluxes remains almost the same, as it varies between 0.1 and 0.2 K , as can be seen in Fig. 3a–d. The reason for this is the low heat flux density, which induces only convective boiling. Higher heat fluxes result in higher amplitudes and frequencies of superheat fluctuations, while higher liquid levels reduce both the amplitude and frequency.

At 1.3 kPa, by increasing the liquid level from 0.57 to 1.89 cm, there was a 24% reduction in nucleation frequency and a 50% reduction in superheat amplitude. At 2.5 kPa superheat fluctuations were suppressed for both analyzed filling levels and all investigated heat flux densities. An increase in liquid level from 0.57 to 1.89 cm resulted in an increase in wall superheat from 16 to 20 K for 1.5 Wcm^{-2} , but a decrease in wall superheat from 56–57 K to 49–50 K for 5.93 Wcm^{-2} .

The small amplitude of wall superheat is due to the fact that the superheat was not sufficient for bubble departure, and thus at both pressures and a heat flux density of 1.5 Wcm^{-2} , the bubbles condensed before reaching the critical diameter. This is analogous to the observations of Tang *et al.* [16] during subcooled boiling at the atmospheric pressure.

The wall superheat for heat fluxes 0.43 Wcm^{-2} and 1.5 Wcm^{-2} decreased by 59% and 41%, respectively, for a 0.57 cm refrigerant level, while increasing the pressure from 1.3 kPa to 2.5 kPa, but for a 1.89 cm refrigerant level, the wall superheat decreased by 57% for the heat flux density 0.43 Wcm^{-2} , 33% for 1.5 Wcm^{-2} and 13% for 5.93 Wcm^{-2} .

In all cases, the application of a heat flux higher than 1.5 Wcm^{-2} enhanced superheat fluctuations. The amplitudes observed in our work did not exceed 2 K, which is significantly below the 25 K observed by Giraud *et al.* [8] at a heat flux of 9.4 Wcm^{-2} and liquid level of 20 cm. It means that we did not reach the conditions for fully developed boiling.

3.3 Jakob number

To confirm that the main mechanism of heat transfer under the measured conditions is not evaporation but convection and heat conduction, the Jakob number was evaluated. The considered mechanisms coincide with the literature data presented by [8].

The Jakob number is a dimensionless determinant of phase heat transfer. It determines the ratio of the sensible to latent heat [7]:

$$\text{Ja} = \frac{\rho_l c_{p(l)} \Delta T_{\text{wall}}}{\rho_v \Delta h_{lv}}. \quad (3)$$

The Jakob number takes the ratio of liquid density to vapour density into account, but under the tested conditions the density of the gas is so small that the aforementioned density ratio would affect the result too much, so it was decided to use a modified Jakob number. It was further modified by

Eq. (4), so as to easily calculate it with the applied heat flux instead of wall superheat [7]:

$$\Delta T \sim \frac{q_{\text{app}} L_c}{\lambda_l}. \quad (4)$$

The outcome is the modified Jakob number Ja^* :

$$\text{Ja}^* = \frac{c_{p(l)} L_c q_{\text{app}}}{\Delta h_{lv} \lambda_l}. \quad (5)$$

3.4 Boiling region map

Figure 4 shows a dimensionless map of boiling regimes, where the values of the modified Jakob number are summarized on the Y axis, and the ratio of vapour pressure to static pressure on the X axis. Dots represent the experimental values we obtained: convection or small popping bubbles and isolated bubble region. As observed by Wojtasik *et al.* [7], by increasing the applied heat flux, first the convection regime and small popping bubbles will appear, and then single non-interacting vapour bubbles can be seen [7].

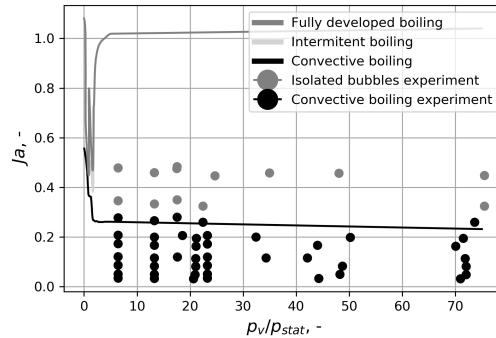


Figure 4: Dimensionless boiling map for subatmospheric pressure (dots) compared with literature data (lines) [7].

The graphs gathered in Fig. 5, showing the dependence of HTC on a given pressure, were used to classify our experimental results. If the data obtained in a given experimental series corresponded to an area of convection (from Fig. 5), they were assigned to the same regime in our dimensionless map (Fig. 4). Received values in our experimental conditions could not be assigned to intermittent boiling or fully developed boiling. Obtaining developed boiling would have occurred at a higher modified Jakob number, i.e. when applying higher heat fluxes.

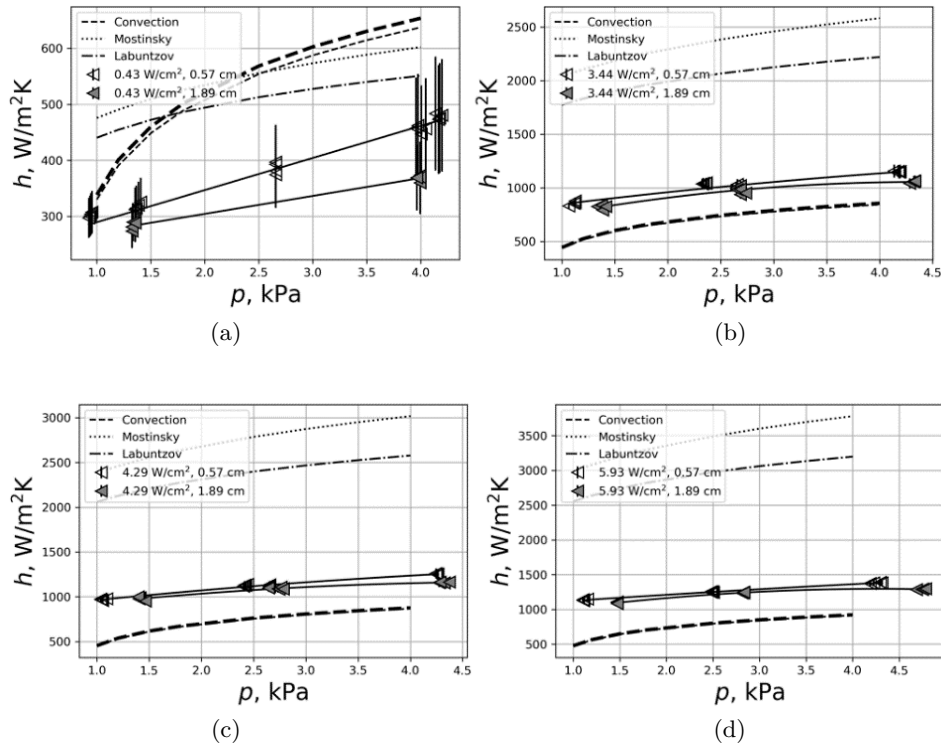


Figure 5: Heat transfer coefficient h as a function of pressure and liquid levels. Heat flux: (a) 0.43 Wcm⁻², (b) 3.44 Wcm⁻², (c) 4.3 Wcm⁻², (d) 5.93 Wcm⁻².

The effect of the ratio of vapour pressure to hydrostatic pressure was studied in the $p_v/p_{stat} > 1$ area. When the vapour pressure is greater than the hydrostatic pressure at low heat fluxes (low modified Jakob number), the occurrence of isolated bubble regimes is achieved more quickly. The higher the hydrostatic pressure (higher liquid level), the greater the subcooling.

The boundary line of interest is the purple line in Fig. 4, corresponding to the modified Jakob number at around 0.3. As the vapour pressure increases, the boundary value of the modified Jakob number, which separates the two regimes observed in the experiment, decreases.

For values around $Ja^* < 0.3$, the dominance of large regions of convection or small popping bubbles is visible, due to a too small applied heat flux. For $Ja^* > 0.3$, the isolated bubble regime dominates. The regions can be confirmed by the wall temperature fluctuations from Fig. 3.

3.5 Heat transfer coefficient

Figure 5 shows the correlation of the heat transfer coefficient with the pressure and refrigerant level. The pressure presented on the x-axis is the total pressure near the heating wall, which is calculated as a sum of pressure at the vapour-liquid interface and hydrostatic pressure. The difference for liquid levels is less than 100 Wm^{-2} , which translates into an up to 10% increase in favour of lower liquid level.

The analysis considers studies for four heat fluxes with values of 0.43, 3.44, 4.3 and 5.93 Wcm^{-2} . The HTC is increasing with pressure at a rate of about $200 \text{ W}\cdot\text{m}^{-2}\text{K}^{-1}$ per 1 kPa. When the heat flux density increases from 0.43 Wcm^{-2} to 5.93 Wcm^{-2} (at about 1 kPa), the heat transfer coefficient also increases from 250 to $1150 \text{ Wm}^{-2}\text{K}^{-1}$. A change in pressure to 4 kPa also results in an increase in the heat transfer coefficient to values in the range of 350 to $1400 \text{ Wm}^{-2}\text{K}^{-1}$ for heat fluxes of 0.43 Wcm^{-2} and 5.93 Wcm^{-2} .

Zajączkowski *et al.* [10] in their article compared sixteen correlations for pool boiling, which are available in the literature. For a subatmospheric pressure, the most accurate approximation of the heat transfer coefficient was obtained using the Mostinski correlation with a reduced pressure and the Labuntsov correlation. These formulas were also used in this work.

The Mostinski formula and the Labuntsov correlation both consider the heat flux density, as in Eq. (6) and (8), respectively:

$$h = 0.00417q^{0.7}p_{\text{crit}}^{0.69}F, \quad (6)$$

where

$$F = 1.8 \left(\frac{p}{p_{\text{crit}}} \right)^{0.17} + 4 \left(\frac{p}{p_{\text{crit}}} \right)^{1.2} + 10 \left(\frac{p}{p_{\text{crit}}} \right) \quad (7)$$

and

$$h = 0.75 \left[1 + 10 \left(\frac{\rho_v}{\rho_l - \rho_v} \right)^{0.67} \right] \left[\frac{k_l^2}{v\sigma(T_{\text{sat}})} \right]^{0.33} q^{0.67}. \quad (8)$$

Based on our previous studies of Zajączkowski *et al.* [10], in dependence of the heat flux, their mean absolute deviation (MAD) ranged from 0.1 to 0.89 for the Labuntsov correlation and from 0.13 to 0.35 for the Mostinsky correlation. For the results examined now, also in dependence of the heat flux, MAD is from 0.36 to 1.38 for the Labuntsov correlation, and from 0.31 to 1.42 for the Mostinsky correlation. Figure 5 presents both the

above-mentioned correlations. The results obtained from our theoretical and experimental investigations have a greater discrepancy. This is most likely because both correlations were designed for fully developed boiling, which we did not obtain in this study. Instead, for the conditions of convective boiling, the heat transfer coefficient h could be calculated from the natural convection formula. For higher heat fluxes, when we reached the isolated region regime, h was between the calculated values of convection and boiling.

Chang *et al.* [17], in their work, experimentally investigated the thermal performance of a two loop thermosyphon in subatmospheric conditions. The working fluid was water in underpressure. This research resulted in three heat transfer correlations by which the heat transfer coefficient over pool boiling, intermittent and vapour regions of the evaporator could be calculated. The pool boiling region was described by Eq. (9):

$$h = \left(1.951 \cdot 10^6 q^{-0.26}\right) P^{(0.508-5.91 \cdot 10^{-6} q)}, \quad (9)$$

where P^* means the dimensionless evaporator pressure, which is a ratio of the evaporation pressure to critical pressure.

This correlation did not work for our experimental data and those calculated by other formulas: the heat transfer coefficient values turned out on average 10 times higher than our values. The reason is that the formula was highly empirical and was proposed for a highly confined evaporator with heating at one of the horizontal walls, much like in plate heat exchangers. This type of heat exchanger is more similar to the one investigated by Sène *et al.* [2]. Sène *et al.* proposed a semi-empirical pool boiling model for confined evaporators, but their formula also is not applicable in our experiments, as it uses the confining thickness parameter, which does not occur in non-confined boiling.

4 Conclusions

In this study, the effect of the refrigerant filling level (0.57–1.89 cm) on the pool boiling heat transfer coefficient h and wall superheat was experimentally explored. Experiments were performed for pressures ranging from 1 to 4 kPa and for heat flux densities ranging from 0.43 to 5.93 Wcm⁻². The results show that under the selected conditions, the impact of liquid level on h is insignificant because an increase of up to 10% for a lower liquid level

was observed, while the measurement error was calculated to be about 12–20%. It was also reported that the difference in the heat transfer coefficient under the same heat flux and pressure conditions near the wall but for different liquid levels is usually less than $100 \text{ Wm}^{-2}\text{K}^{-1}$. The heat transfer coefficient increase with pressure is about $200 \text{ Wm}^{-2}\text{K}^{-1}$ per 1 kPa.

For the lowest measured heat flux, the superheat is generally greater than 10 K under examined conditions, which is the biggest drawback of flooded evaporators.

The paper also highlights the dependence of wall superheat fluctuations on boiling dynamics. In the conditions we studied, small fluctuations were observed, as they were caused by nucleation and the fluid motion that result from boiling.

The mechanism of boiling at subatmospheric pressure looks different from that at the atmospheric pressure. With different liquid levels, the difference in heat transfer is noticeable only in the region of convective boiling, while its shift to nucleation boiling is moved toward a higher wall superheat. Because as the liquid height increases, the pressure at the wall also increases, lower filling levels are advisable for water under a subatmospheric pressure.

Under the given conditions, the dominant mechanisms of heat transfer are both heat convection and conduction, instead of evaporation. For values of $Ja^* < 0.3$, the dominance of convection or small popping bubbles is visible, due to low applied heat flux. For $Ja^* > 0.3$, the isolated bubble regime dominates. We did not reach other boiling regimes in this study.

Received 13 April 2023

References

- [1] Sikora M., Bohdal T.: *New environmentally friendly low-pressure refrigerants mini-channel*. Arch. Thermodyn. **44**(2023), 1, 89–104.
- [2] Sène P., Giraud F., Sow M.L., Tréméac B.: *Heat transfer coefficient correlations of water subatmospheric vaporization in a channel of a smooth plate heat exchanger, based on Vaschy-Buckingham theorem*. Appl. Therm. Eng. **213** (2022), 1–17.
- [3] Schnabel L., Scherr C., Webe, C.: *Water as refrigerant- experimental evaluation of boiling characteristics at low temperatures and pressures*. In: Proc.VII Minsk Int. Sem. Heat Pipes, Heat Pumps, Refrigerators, Power Sources, Minsk 2008, 322–330.
- [4] Schultz K.: *Configured Surface Tubes for Evaporation of Water*. In: Proc. Int. Sorption Heat Pump Conf. Broomfield, 2005, 271–279.

- [5] Herold K.E., Radermacher R., Klein S.A.: *Absorption Chillers and Heat Pumps*. CRC, Boca Raton 1996.
- [6] Michaiie S., Rullière R., Bonjour J.: *Towards a more generalized understanding of pool boiling at low pressure: Bubble dynamics for two fluids in states of thermodynamic similarity*. Exp. Therm. Fluid. Sci. **101**(2019), 217–230.
- [7] Wojtasik K., Rullière R., Krolicki Z., Zajaczkowski B., Bonjour J.: *Subcooled boiling regime map for water at low saturation temperature and subatmospheric pressure*. Exp. Therm. Fluid. Sci. **118**(2020), 1–11.
- [8] Giraud F., Rullière R., Toublanc C., Clausse M., Bonjour J.: *Experimental evidence of a new regime for boiling of water at subatmospheric pressure*. Exp. Therm. Fluid. Sci. **60**(2015), 45–53.
- [9] Halon T., Zajaczkowski B., Królicki Z., Wojtasik K.: *Calculation and experimental verification of heat transfer coefficient for low pressure methanol evaporator*. In: Proc. 24th Int. Cong. of Refrigeration, Yokohama, August 16-22, 2015, 1–8.
- [10] Zajaczkowski B., Halon T., Krolicki Z.: *Experimental verification of heat transfer coefficient for nucleate boiling at sub-atmospheric pressure and small heat fluxes*. Heat Mass Transfer **52**(2016), 205215.
- [11] Bell I.H., Wronski J., Quoilin S., Lemort V.: *Pure and pseudo-pure fluid thermophysical property evaluation and the open-source thermophysical property library coolprop*. Ind. Eng. Chem. Res. **53**(2014), 6, 2498–2508.
- [12] Thome J.R.: *Boiling*. In: Heat Transfer Handbook Handbook (A. Bejan, A.D. Kraus, Eds.), Wiley Hoboken 2003, 635–717.
- [13] Giraud F., Rullière R., Toublanc C., Clausse M., Bonjour J.: *Preliminary experimental investigation on water boiling phenomena in a liquid layer at subatmospheric pressure*. In: Proc. 24th Int. Cong. of Refrigeration (ICR 2015), Yokohama, 2015.
- [14] Shen B., Mine T., Iwata N., Hidaka S., Takahashi K., Takata Y.: *Deterioration of boiling heat transfer on biphilic surfaces under very low pressures*. Exp. Therm. Fluid Sci. **113**(2020), 110026.
- [15] Zimmermann M., Heinz M., Sielaff A., Gambaryan-Roisman T., Stephan P.: *Influence of system pressure on pool boiling regimes on a microstructured surface compared to a smooth surface*. Exp Heat Transfer **33**(2019), 4, 318–334.
- [16] Tang J., Zhu G., Sun L.: *Microbubble emission boiling in subcooled pool boiling and the role of Marangoni convection in its formation*. Exp. Therm. Fluid Sci. **50**(2013), 97–106.
- [17] Chang S., Lo D., Chiang K., Lin C.: *Sub-atmospheric boiling heat transfer and thermal performance of two-phase loop thermosyphon*. Exp. Therm. Fluid Sci. **39**(2012), 134–147.